

# High $p_T$ QCD Physics Results from the Tevatron

Raymond Brock

*Department of Physics and Astronomy, Michigan State University, East Lansing, MI 48824, USA*

The dominant QCD physics results from the Fermilab Tevatron Collider are reviewed. Special attention is paid to direct photon experiments and their analysis and inclusive jet cross sections. Model dependence in the interpretation of experimental results is emphasized, especially with regard to the recent inclusive jet cross section measurements.

## 1 Introduction

QCD physics at the Tevatron has become a mature subject with a number of measurements reported at this conference by representatives of the two collider experiments, CDF and DØ. Most of the results come from the nearly four years of running at the Tevatron, called Run 1. These data were taken in three distinct periods with the second run's accumulated luminosity totaling 7-8 times more than either the first or last runs. While the nominal running is at a center of mass energy of 1800 GeV, there was a short period of 630 GeV running for primarily QCD topics. Table 1 shows the luminosity distribution among the three running periods. Run 1A was the first exposure of the DØ detector to beam.

The result has been enormous data sets for QCD physics study with final states which include multiple jets, isolated photons, and  $W$  and  $Z$  bosons. With these data, precision comparisons are possible with predictions of perturbative quantum chromodynamics (pQCD), primarily at next to leading order (NLO). Both experiments use similar selection criteria in order to isolate these final states of interest. Unless otherwise noted, these criteria include those characteristics outlined in table 2.

Often reviews of this sort are called "Tests of QCD". However, in order to make a point later, this broad subject has been broken up into three sub-units: measurements which can Characterize Data, Challenge Theory, and Confront Models. That such a division is now possible is a credit to Fermilab, the experimental collaborations, and the theory community. As we'll see, these are detailed and complex experiments with increasingly impressive import.

A theme will run throughout this review. Literally and figuratively, the ingredient which "holds

Table 1: Accumulated running for the 1992-1995 period as recorded by the DØ experiment (CDF totals are approximately 10% higher).

Run	$\sqrt{s}$ GeV	Years	$\int \mathcal{L} dt$ pb $^{-1}$
1A	1800	1992-1993	$13.5 \pm 0.7$
1B	1800	1994-1995	$85.2 \pm 4.6$
1C	1800	1995-1996	$\sim 10$
1C	630	1996	$\sim 0.5$

it all together" is the gluon. We will see that perhaps it is not as well known as originally thought and that gluon resummation may prove to be the major hurdle. As such, resummation may prove to be one of the major experimental and theoretical challenges between now and the next installment of this conference.

## 2 Characterization of Data

A variety of measurements are traditionally used to provide data which can be parameterized with the help of a NLO pQCD model. Paradigm examples of such measurements are cross section determinations (which have inherent as well as subsidiary importance) and the various inputs to global parton distribution function (pdf) fits. In this latter exercise, data from the Tevatron are only just beginning to be useful. More influence, on particularly the gluon distribution, is guaranteed as these high quality data become better understood.

### 2.1 $W$ Charge Asymmetry

A mature program which characterizes data appropriate for pdf input is that of CDF<sup>1</sup> which measures the rapidity dependence of the charge asymmetry for  $W$  bosons from the reaction  $p\bar{p} \rightarrow$

Table 2: General requirements for objects of QCD study as defined by CDF and DØ. Incremental differences from these values will be noted in the text. (“em” stands for “electromagnetic”.)

object	primary characteristic
<b>jets</b> fixed cone algorithm	$\Delta R = 0.7$ $E_T^j > 15 \text{ GeV}$
<b>photons</b> isolated em cluster	$E_T^\gamma > 12 \text{ GeV}$
$W(Z)$ isolated em cluster(s)	$E_T^\ell > 20 \text{ GeV}$ $\cancel{E}_T > 20 - 25 \text{ GeV}$
<b>acceptance:</b> jets em objects	$-3.5 < \eta < 3.5$ $-1 < \eta < 1$

$W^\pm X$ . Particular interest is paid to this set of measurements because of the nearly unique effect that they have on constraining pdf fits at  $q \sim M_W$ . In particular, the constraint is on the *slope* of the  $u(x)/d(x)$  ratio, not just its absolute value. There are two components of the measured asymmetry, one due to production and second due to the parity-violating decay. The measurable is the lepton rapidity from  $p\bar{p} \rightarrow \ell^\pm X$ , or specifically

$$A^W(y) = \frac{\frac{d\sigma^+}{dy_\ell} - \frac{d\sigma^-}{dy_\ell}}{\frac{d\sigma^+}{dy_\ell} + \frac{d\sigma^-}{dy_\ell}}. \quad (1)$$

Here,  $\sigma^{+(-)}$  refers to the cross section for antilepton (lepton) production. Clearly, determination of the lepton electric charge is necessary which, for electrons, requires a central magnetic field. The earliest CDF Run 1A data of  $20\text{pb}^{-1}$  were instrumental in discriminating among competing pdf sets, namely MRSB<sup>4</sup>, MRSDO<sup>5</sup>, and CTEQ2M<sup>6</sup>.

At this conference, new data were presented by the CDF collaboration for  $91\text{pb}^{-1}$  from Run 1B for  $p\bar{p} \rightarrow W(e \text{ or } \mu)\nu X$ .<sup>2</sup> These data have doubled in the forward region,  $1.2 < y_\ell < 1.8$  due to the incorporation of forward tracking and the plug calorimeter. Figure 1 shows these new data compared with the perturbative DYRAD calculation<sup>3</sup> for muons and electrons combined. For both leptons, the requirements were that  $p(\ell), p(\nu_\ell) > 25 \text{ GeV}/c$ . Two recent pdf sets, MRSA<sup>7</sup> and CTEQ3M<sup>8</sup>, are shown along with older sets.

The DØ collaboration<sup>11</sup> has also presented

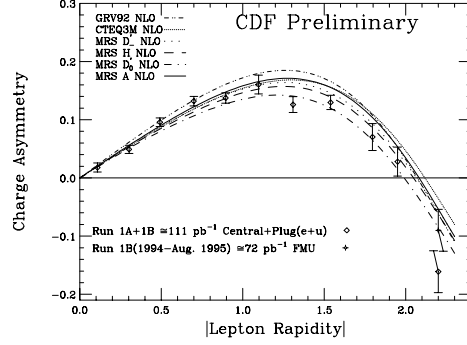


Figure 1: Comparison of the CDF charge asymmetry measurement with modern pdf sets. The data include the Run 1A central and plug input as well as the Run 1B central+plug sets.

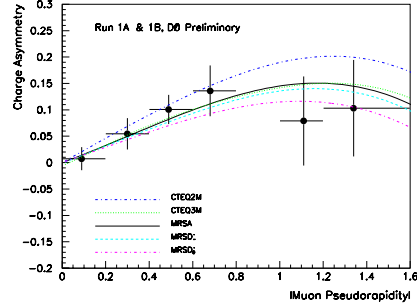


Figure 2: Preliminary measurement of  $W$  charge asymmetry as determined from muons by the DØ collaboration. The curves are predictions of the single production model due to Ladsinsky and Yuan for different pdf's.

the first results for  $A^W(y)$  with muon final states. These data are for the Run 1B exposure and require that  $p_T(\mu), p_T(\nu) > 20 \text{ GeV}/c$ . These data are from the central,  $|\eta| < 1.0$  ( $\sim 55\text{pb}^{-1}$ ), and forward,  $1.0 < |\eta| < 1.7$ , ( $\sim 35\text{pb}^{-1}$ ) regions requiring a single muon trigger. The detector asymmetries are largely compensated for by reversing the polarity of the toroidal magnets on a weekly basis. The remaining small asymmetry inherent in the detector,  $\sim 3\%$  ( $\sim 6\%$ ) of the total luminosity in the forward (central) regions, is corrected for in the measurement.

The model comparisons in Figure 2 use the results of a full gluon resummed<sup>12</sup> program, RESBOS<sup>13</sup>. Interestingly, Figure 3 shows the CDF data compared to predictions of both the DYRAD and RESBOS generators, where the former is a perturbative calculation. Not only does RESBOS

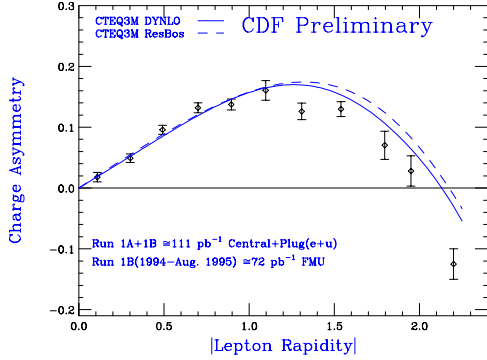


Figure 3: Comparison of the CDF charge asymmetry measurements with two models, DYRAD and one which includes a gluon resummation (RESBOS)

incorporate the gluon resummation phenomenology, but it also includes the full  $W$  density matrix. Both calculations use the same pdf, CTEQ3M. There are small differences between the two and it is not clear what might account for them—note also that neither agrees well with the data at the higher rapidities. These data are becoming increasingly precise and one wonders whether  $A^W(y)$  might be useful in the future in extracting information about the non-perturbative parameterization which is inherent in the implementation of the resummation prescription and which has originated largely from rather old Drell-Yan experimental data<sup>14</sup>.

The particular interest in these measurements is the pdf constraint, which is most relevant in the determination of the model uncertainties in the measurement of  $M_W$ , which currently stands at approximately  $\pm(50 - 60)\text{MeV}/c^2$ . While the modeling of the  $p_T^W$  distribution is a major component of the model uncertainty (related to the sum of pdf's), the asymmetry too makes a significant, direct contribution to this understanding (as related to the difference of pdf's).  $A^W(y)$  is the only such input to the global fitting which takes place at the  $Q$  and  $x$  appropriate to  $W$  production and hence  $M_W$  determination.

## 2.2 $W$ and $Z$ Boson Cross Sections

Another standard measurement on a menu of collider QCD physics is the determination of the total cross sections for the production of the heavy intermediate vector bosons (ivb),  $\sigma_W$  and  $\sigma_Z$ . These measurements are fundamental in their own right, but also important as among the primary measur-

ables which combine with other data and pQCD to extract the  $W$  width,  $\Gamma(W)$ . Both experiments have published Run 1A measurements (DØ<sup>9</sup>, CDF<sup>10</sup>). At this conference, DØ reported preliminary measurements<sup>11</sup> for Run 1B for cross sections times the relevant leptonic branching ratios and the ratios of these quantities for  $W$  and  $Z$ .

The standard DØ isolated central lepton selection criteria are used with  $p_T(e), \cancel{E}_T > 25$  GeV and  $p_T(\mu), \cancel{E}_T > 20$  GeV. The  $W(Z)$  electron measurement comes from  $75.9 \pm 6.4$  pb<sup>-1</sup> ( $89.1 \pm 7.5$  pb<sup>-1</sup>), while the  $W$  and  $Z$  muon measurements come from  $32.0 \pm 2.7$  pb<sup>-1</sup>. These preliminary results are:

$$\begin{aligned}\sigma_W B(e\nu) &= 2.38 \pm 0.01 \pm 0.09 \pm 0.20 \text{ nb}, \\ \sigma_W B(\mu\nu) &= 2.28 \pm 0.04 \pm 0.16 \pm 0.19 \text{ nb}, \\ \sigma_Z B(ee) &= 0.235 \pm 0.003 \pm 0.005 \pm 0.020 \text{ nb}, \\ \sigma_Z B(\mu\mu) &= 0.202 \pm 0.016 \pm 0.020 \pm 0.017 \text{ nb}.\end{aligned}$$

Almost all of the systematic uncertainties are uncorrelated among the measurements, facilitating their combination. The preliminary result for their combined ratio is  $R_{\ell=e+\mu} \equiv \sigma_W B(\ell)/\sigma_Z B(\ell\ell) = 10.32 \pm 0.43$ . With a partial width calculation of  $\Gamma(W \rightarrow e\nu) = 225.2 \pm 1.5$  MeV, this leads to a preliminary result for the  $W$  width of  $\Gamma(W) = 2.159 \pm 0.092$  GeV. This is in agreement with the Standard Model prediction of  $\Gamma(W) = 2.077 \pm 0.014$  GeV

## 3 Challenging pQCD

While pQCD is very successful in understanding many of the details of hadronic physics, there are corners of this field which are now undergoing deeper investigation, driven by data. These areas of concentration were actually anticipated theoretically, but it is only in recent years that measurements have begun to reach the precision and accuracy sufficient to actually challenge pQCD. In point of fact, this challenge is actually in the region between the strict application of the perturbative region and the non-perturbative region, a subject of great complexity (and confusion) for many years. Increasingly, the need for an applicable description for multiple soft gluon production is becoming apparent, in both the high and the low  $x$  regimes. The challenges come from top production<sup>15</sup>, Drell-Yan production (although neither Tevatron experiment has yet presented high

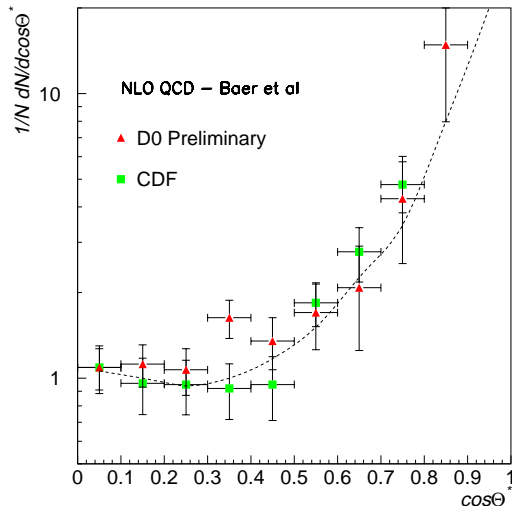


Figure 4: DØ and CDF normalized center of mass angular distributions for photons relative to the jet direction as compared to a NLO prediction.

statistics continuum Drell Yan or  $Z$  cross sections), and direct photon production. A unified, applicable phenomenology only exists<sup>12 16 14</sup> for Drell-Yan production where the two scale nature of the problem drew initial attention.

### 3.1 Direct Photon Production

The determination of the inclusive cross section for direct photon production has long been understood to be the primary ingredient necessary to constrain and characterize the gluon parton density which is presumed to be parameterized as

$$G(x) \sim x^A (1-x)^B f(x). \quad (2)$$

Here,  $f(x)$  is a term inserted for flexibility in the global fitting... usually with one or two parameters. As the data have improved, the ability to measure double differential cross sections and correlations among the photon and jets or even two photons became possible. Figure 4 shows both the DØ and CDF angular distribution of the photon relative to the jet directions and a NLO prediction<sup>19</sup>.

One of the difficulties in global analyses using direct photon data is that while the half dozen experiments together cover a range in  $x$  from 0.01–0.5, individual experiments are limited in their

range to only a couple of tenths, or less. These cross section measurements have possibly begun to show hints of deviation from the predictions. This is true of the current collider experiments (and, in retrospect, those of the previous generation) as well as the Fermilab fixed target experiment, E706.

Both CDF<sup>17</sup> and DØ<sup>18</sup> have statistically identified large samples of relatively pure, central, isolated direct photon events. These samples are difficult to distinguish from electroweak and jet backgrounds production, without severe cuts on  $\cancel{E}_T$  and isolation. In both experiments, samples which are pure at the level of 25%(80%) for  $p_T^\gamma < 20(60)$  GeV/c are obtained and were reported at this conference. These large samples have begun to show hints of deviations from expectations at the lower  $p_T^\gamma$  regions, below  $\sim 30$  GeV/c. While there are continued concerns about the definition of the renormalization scale, both experiments and predictions consistently choose  $\mu = p_T^\gamma$ .

Figures 5 and 6 show the inclusive cross sections from both collider experiments for the same pdf model and scale definitions. The two experiments draw different conclusions from these data, CDF<sup>17</sup>: "...excess at low end seems to require internal  $k_T$ ..." and DØ<sup>18</sup>: "...large systematic errors...prohibit any conclusive statement at this time...". Figure 7 shows the quantity (data – model)/model ( $\equiv [D - M]/M$ ) for the DØ data as well as the  $1\sigma$  correlated systematic errors which indeed point out that the systematic understanding is compromised in the suspicious region. The CDF correlated systematic uncertainties at  $p_T^\gamma \sim 10$  GeV/c are approximately 10-12% and relatively flat.

Such an effect has been around for a long time. Figure 8 shows a similar effect<sup>20</sup> as a deviation in the regions of  $x_T = 2p_T^\gamma/\sqrt{s}$  covered by each of the experiments. These are difficult systematic regions as all refer to  $p_T^\gamma \sim 5$  GeV/c or so. This effect is qualitatively reminiscent of the region of  $p_T^W$  which is most affected by the incoherent emission of soft gluons. Indeed, the process  $p\bar{p} \rightarrow W(Z)X$  shares obvious common features with  $p\bar{p} \rightarrow \gamma X$  (except for the important differences of the fixed mass scale for the ivb case).

It seems that the deviation from pQCD expectations can be reduced or eliminated by the presumption of an inspired choice of primordial  $k_T$ . For example, application of a  $\sqrt{s}$ -dependent  $k_T$  to

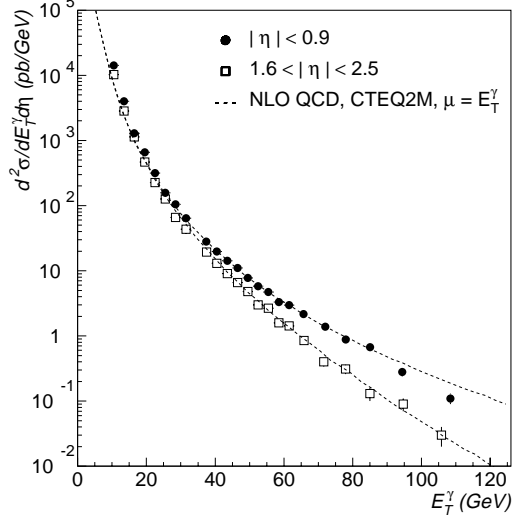


Figure 5:  $D\bar{O}$  inclusive cross section for direct photon production from the Run 1A running period.

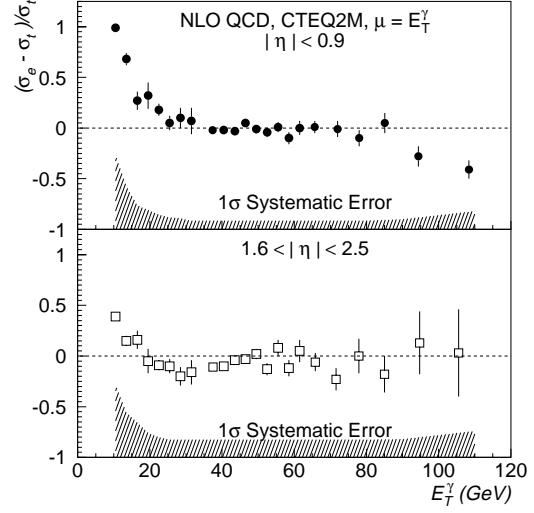


Figure 7:  $D\bar{O}$   $[D - M]/M$  inclusive cross section. The lower figure shows the first measurement in the forward region.

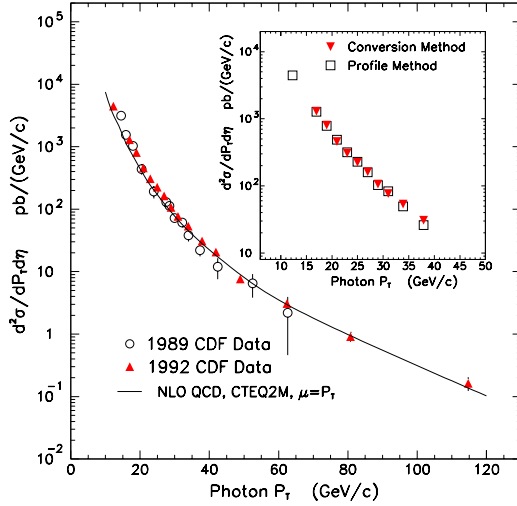


Figure 6: CDF inclusive cross section for direct photon production from the 1989 and Run 1A running periods. The inset shows the comparison of two different photon identification techniques.

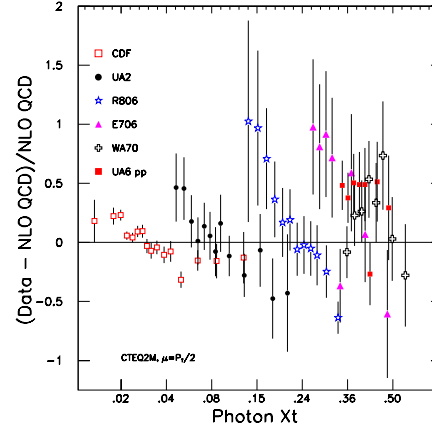


Figure 8:  $[D - M]/M$  for a variety of fixed target and collider direct photon experiments demonstrating a pattern in their deviation from the perturbative expectation.

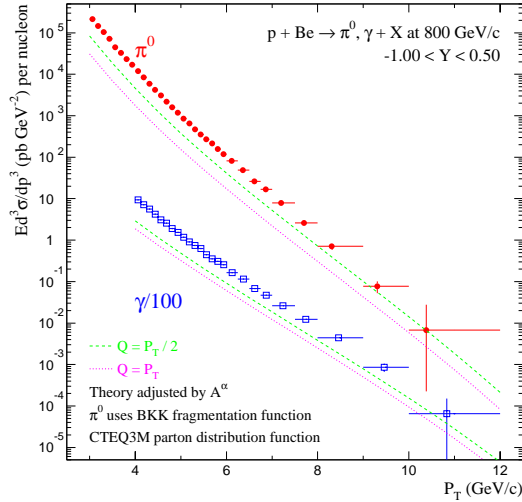


Figure 9: E706 invariant inclusive cross section for photon and  $\pi^0$  production for protons of 800 GeV/c on a Be target. The curves show the prediction for two values of the scale. An addition of a primordial  $k_T \sim 1.4$  GeV/c results in agreement.

each of the experiments in Figure 8 eliminates the systematic disagreement with the model<sup>20</sup>. However, incorporation of these effects in a useful way requires a monte carlo shower program.

Recently there was an attempt to incorporate a shower algorithm in an “Owens-like” monte carlo by adjusting the algorithmic cut-off parameters for emission<sup>21</sup>. While this was successful for the CDF data, it fails for ISR and UA2 data. Is this a problem which can be solved by a consistent resummation phenomenology? It is worth noting that this kind of problem has been around for many years and was first noted by WA70 in diphoton data in 1990<sup>22</sup> which found that  $k_T \sim 0.9$  GeV/c was necessary to match their data with NLO predictions for diphoton production. The most recent observation of this is by the E706 collaboration at Fermilab<sup>23</sup>. Figure 9 shows the direct photon data from their  $p - Be$  exposure at  $p_p = 800$  GeV/c. The observed deviation is almost completely removed by the application of  $k_T \sim 1.4$  GeV/c. Finally, while clearly a final state radiation phenomenon, it is maybe amusing to note that OPAL<sup>24</sup> has presented preliminary data for direct photon data in  $e^+e^- \rightarrow \gamma X$  which also disagree with pQCD expectations of final state gluon

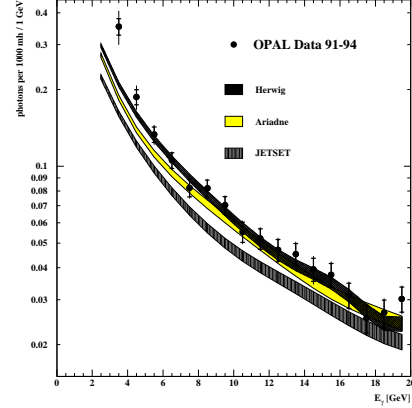


Figure 10: Energy distributions of isolated final state photons after background subtractions and efficiency corrections. The model predictions have been smoothed.

emission for  $p_T^\gamma \sim 2 - 5$  GeV/c. Figure 10 shows this deviation from expectations at low  $E_\gamma$ .

### 3.2 Diffractive Scattering and Rapidity Gaps

The field of diffractive scattering, or “hard” diffractive scattering is clearly undergoing a renaissance. The question of an isolated exchange of vacuum quantum numbers in a form which appears to be coherent enough to be given a name (“pomeron”) has become fashionable again with growing supportive evidence that this picture is correct. This conference saw reports from CDF and DØ for new results and updates of previously published results. These are complicated analyses and are similar in many respects. As a mnemonic, it is useful to keep track of the different processes with cartoons or icons which represent the general jet and gap structure in  $\eta - \phi$  plots. For this purpose, we’ll represent them as in-line icons:  $[a|b|c]$ , where the regions between the vertical lines indicate generally “forward” ( $a$  and  $c$ ) and “central” ( $b$ ) regions. In this nomenclature a rapidity-plateau event might be represented by  $[j|j|j]$ , indicating that jets may be produced at largely any rapidity. With this scheme, then the processes of interest are:

DS  $[| | |]$  Diffractive Scattering. In such triggers, essentially no activity is seen as a pomeron is lightly exchanged between the in-

coming and intact outgoing  $p$  and  $\bar{p}$ , which escape. Little or no energy deposition is observed in such events.

**HSD**  $[\mid \mid \mid jj]$  Hard Single Diffraction. Here, a single pomeron exchange breaks up one of the protons into two same side jets which are produced in conjunction with an opposite, forward rapidity gap.

**HDPE**  $[\mid \mid jj] \mid$  Hard Double Pomeron Exchange. Here, two pomerons are emitted and annihilate centrally into two jets leaving two forward gaps.

**Diff W**  $[\mid \mid Wj] \mid$  If the pomeron has an explicit parton content, a quark from it could annihilate with a quark from one of the protons into a  $W$  and a jet.

**HCSE**  $[\mid j \mid \mid j]$  Hard Color Singlet Exchange.

Here, a pomeron is exchanged between the  $p$  and  $\bar{p}$  which break up into forward jets, leaving no hadronic production centrally.

The new and updated results at this conference were for HSD, HDPE, and HCSE reactions.

### 3.3 HSD: $[\mid \mid \mid jj]$

Hard diffractive processes have been observed in many contexts at CERN and the Tevatron. The signal for HSD is the presence of a rapidity gap, a lack of particles in a broad range of rapidity co-incident with evidence that a hard scattering had occurred.  $D\bar{O}$  presented data at this conference which showed evidence for HSD scattering into two high  $E_T$  jets. The trigger was two jets both of  $E_T > 12$  GeV in either the forward,  $\eta > 1.6$  or backward,  $\eta < -1.6$  regions. These data have been collected in both the  $\sqrt{s} = 1800$  GeV and the Run 1C,  $\sqrt{s} = 630$  GeV running. Figure 11 shows the results of the “zero track” distribution for the high energy running (top) and the low energy running (bottom).

CDF also presented results from a search for dijet events which requires  $|\eta| > 1.8$  for the pair and  $20 < E_T < 60$  GeV for each jet. In the opposite forward direction ( $2.0 < \eta < 4.2$ ) no low multiplicity signal was observed and so a limit on HSD was set at  $< 1.75\%$  (95% CL).

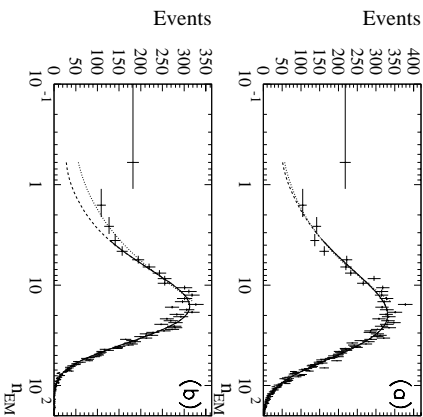


Figure 11: Number of electromagnetic calorimeter towers ( $\eta_{EM}$ ) above a 200 MeV energy threshold in the forward region,  $2 < \eta < 4.1$ , opposite the two jets. The curves are negative-binomial fits to the data. The bottom figure is from Run 1C.

### Hardware Triggering for Diffractive Events

At this conference, CDF presented initial evidence that a hardware diffraction trigger was successful. This was constructed for use in the few months of the 1C running period and used trigger scintillators and  $x-y$  position fiber detectors. These were positioned in three “roman-pot” stations slightly off the central momentum trajectory 55m downstream of the CDF detector in the antiproton direction. Slightly scattered  $\bar{p}$  (in which the antiproton loses 90 to 94% of its momentum) are bent off-axis by the Tevatron dipoles and detected. The full analysis of these 1.2M triggers is in progress, but preliminary indications are that within the roman-pot trigger sample which then enforces a forward rapidity gap presence, 616 dijet events were collected. The preliminary rate suggests a cross section for HSD production of  $\sim 0.6\mu b$ .

### 3.4 HDPE: $[\mid \mid jj] \mid$

$D\bar{O}$  has also implemented a gap-trigger which vetoed deposition in the Level 0 trigger counters which are forward along each beam direction. With an enhanced data set of gap events, an opposite forward gap was searched for in coincidence with two central ( $\eta < 1.0$ ) jets. A clear sample of double-gap events with central jets is seen above background. However, their interpretation as Hard Double Pomeron Exchange examples is not yet clear.

### 3.5 HCSE: $[j] \quad [j]$

A central rapidity gap which is bracketed by two single jets, each in opposite forward directions, is a signal for the exchange of a color-singlet (“colorless”) object. In  $D\bar{O}$  dijet samples with identical kinematical quantities, except for the sign of the quantity  $\hat{\eta}_1^j \cdot \hat{\eta}_2^j$  are used. For the positive sign, the jets are presumably conventional color-exchange sources. For the negative sign, the jets are on opposite sides and a signal for HCSE. The former serves as a background measure for the latter. The resulting signal above background was determined in Run 1A to be  $1.07 \pm 1.10^{+0.25}_{-0.13}\%$  where the first uncertainty is statistical and the second is systematic. This cannot be explained by electroweak exchange. At this conference, new data from the Run 1B exposure were presented which are more precise. They were taken with a variety of triggers which were meant to allow the measurement as a function of  $\eta$  separation and  $E_T^j$ . While the overall signal strength is consistent with the previous measurement, it appears constant over a wide range of  $E_T^j$  in spite of the drastically falling dijet cross section.

CDF similarly searched for dijet events in which the two jets are required to be in opposite hemispheres,  $|\eta| > 1.8$ , for  $E_T > 20$  GeV. By using the track multiplicity between these jets and a normalization from the same side jets, a clear signal is found with low or zero multiplicity. The level of the CDF signal for HCSE is  $2.0 \pm 0.7\%$ .

## 4 Confrontation with Models

Many measurements don’t immediately challenge pQCD theory. Rather, sometimes as a prelude to an eventual theory challenge, such experimental results confront the **implementation** of pQCD theory through models, referred to in this review as “M”.

### 4.1 $W$ Plus Jets

The measurement of the ratio of cross sections,  $\mathcal{R}^{10} = \sigma(W + 1 \text{ jet})/\sigma(W + 0 \text{ jets})$ , has been traditionally<sup>25</sup> used as a measurement of  $\alpha_S(M_W^2)$ . Such a measurement relied on tree-level models which originally used K-factor corrections, rather than NLO predictions. There appeared to be sufficient variation in  $\mathcal{R}^{10}$  as a function of  $\alpha_S$  to find

a solution.

Using the Run 1B data set, the  $D\bar{O}$  collaboration<sup>26</sup> has presented a preliminary determination of  $\mathcal{R}^{10}$ . The analysis utilizes standard selection criteria for  $W$  bosons as well as a 25 GeV/c minimum on jet  $E_T$ . The primary background is from events which fake a  $W^\pm \rightarrow e^\pm \nu$  reaction, which are electromagnetic fluctuations within hadronic showers, a background of 1.6% (6.8%) for  $W + 0$  jets ( $W + 1$  jet). There is an overall 2% background from all other sources. The preliminary measurement of this quantity is  $\mathcal{R}^{10} = 0.079 \pm 0.002 \pm 0.005$  where the second uncertainty is systematic and dominated by the jet energy scale.

There are two related surprises in the interpretation of this result. First, to predict  $\mathcal{R}^{10}$  as a function of  $\alpha_S$ , it is necessary to refit the pdf’s to incorporate the subsequent change in  $\Lambda_{QCD}$ . This appears to remove any  $\alpha_S$  dependence of  $\mathcal{R}^{10}$  over a wide range. In effect, inclusion of  $\alpha_S$  in both the matrix element and the pdf’s appears to cancel the anticipated effect. The second surprise is that the DYRAD expectation for this quantity is not only constant, but considerably lower,  $\mathcal{R}^{10}(\text{DYRAD}) \sim 0.06$ . When both the  $D\bar{O}$  and the UA2 analyses are compared for the case in which the  $\alpha_S$  variation is in the matrix element only,  $\mathcal{R}^{10}$  increases, however less for  $D\bar{O}$  than for UA2.

A speculation is that the  $x$ -range difference between the CERN collider and the Tevatron would be responsible for enhanced quark-gluon initial state annihilation. The uncertainty in the gluon distribution allows  $\Lambda_{QCD}$  to change considerably. In turn, because the Tevatron kinematics favor gluon annihilation more than at CERN, there is a greater effect as different values of  $\alpha_S$  are tested...this gluon effect appears to cancel and flatten the prediction.

### 4.2 “Color Coherence”

One of the difficulties in modeling gluon emission in hadron collisions is the necessity of accounting for gluon interference effects, so-called Color Coherence. While complicated in any case, implementation in simulation of hadron collisions is especially problematic. This is typically accomplished in the full-shower monte carlos by implementing an “angular ordering” (AO) in the emission angles of successively radiated gluons. The



presence of radiative effects from both the initial and final colored states in a hadron collider complicates the situation in general, and specifically includes initial and final state interference. All of this must be taken into account in the shower monte carlos.

Color coherence had been previously observed at the Tevatron<sup>27</sup>. The DØ collaboration<sup>28</sup> reported on updates of their results for multijet events and preliminarily reported on results in events with (colorless)  $W$  bosons.

Three jet events are used to isolate a measurable which tests various models for these effects. This measurable is an angle in  $\eta - \phi$  space,  $\beta$ , which is the angle of  $j_3$  relative to the proton direction, about an axis which is centered on  $j_2$ . (Here,  $E_T(j_1) > E_T(j_2) > E_T(j_3)$ .) The ratio of data to monte carlo, is then plotted as a function of  $\beta$  for these events. If there is no angular ordering in the model, this ratio will peak at  $\beta = 0, \pi$ , and  $2\pi$  and dip at  $\beta = \pi/2$  and  $3\pi/2$ . Figure 12 shows this ratio for ISAJET (which does not implement an angular ordering), HERWIG (which does), and PYTHIA (in which angular ordering can be switched on and off). One can readily see that HERWIG and PYTHIA reproduce the data for this effect. It is also interesting that the  $\mathcal{O}(\alpha_S^3)$  program, JETRAD<sup>39</sup> agrees with data as well.

The  $W$  boson, as a colorless object, will not necessarily be accompanied by particle production, and as such it can be used as a normalization of a region which should be free of gluons. The  $W \rightarrow e\nu$  events are used, with the direction of the  $W$  boson inferred from the preferred solution to the two-fold rapidity ambiguity in the  $W$  rapidity. (This is a standard situation, with the smaller  $\eta_\nu$  of the possible solutions preferred 2/3 of the time.) Annular regions are constructed around both the  $W$  direction and the opposite jet direction, with the angle around each determined as before. As before, there is clear structure in the angular distributions, peaking in the event plane precisely as predicted by models which incorporate an AO algorithm. This is clearly a case in which gluon physics is well represented by models.

### 4.3 Fragmentation

Another of the standard studies in  $e^+e^-$  experiments is the fragmentation of hadrons. Measurements of mean charged multiplicities as a func-

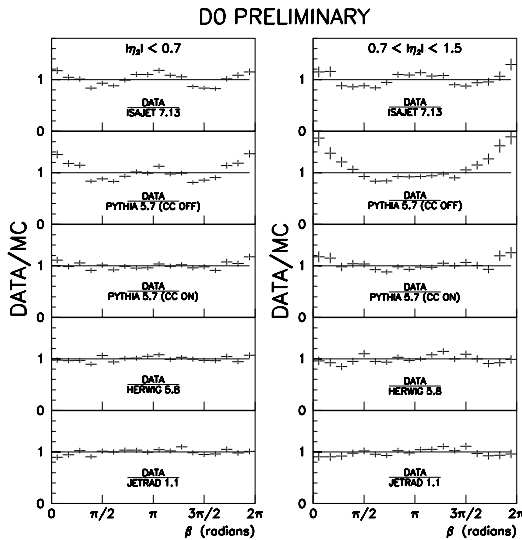


Figure 12: Angular distributions for the ratio of data to various monte carlo models as a function of the angle  $\beta$  defined in the text. Notice that for models which do not have AO (Isajet and PYTHIA with it explicitly disabled), there is poor agreement. For models which do implement an AO algorithm (HERWIG and PYTHIA), the structure is similar in data and monte carlo. The  $\mathcal{O}(\alpha_S^3)$  program, JETRAD agrees with data as well.

tion of  $E_T^{jet}$ , fragmentation functions in the scaling variable,  $x_p$  ( $x_p = 2p/\sqrt{s}$ , where  $p$  is the particle momentum), determinations of  $\alpha_S$ , jet shapes, etc. are all of very high quality and compare favorably with predictions, such as those of JETSET. Especially noteworthy (for a hadron physicist!) is the ability to reliably separate quark from gluon jets.

One standard measurable is that of the peak position of the distribution,  $1/\sigma d\sigma_{ch}/d\xi_p$ , where  $\xi_p = 1/x_p$ . At this conference, there were preliminary results shown of the very recent LEP 2 running at  $\sqrt{s} = 161$  GeV. Figure 13 shows new data<sup>29</sup> with  $\int \mathcal{L} dt = 2.55 \text{ pb}^{-1}$  at  $\sqrt{s} = 161$  GeV with a fit of the peak,  $\xi^* = 4.05 \pm 0.06 \pm 0.09$ , showing that the charged tracks carry roughly a quarter of the available momentum. Good agreement with PYTHIA is apparent. Note also a NLLA<sup>30</sup> fit does well.

An impressive fragmentation analysis was pre-

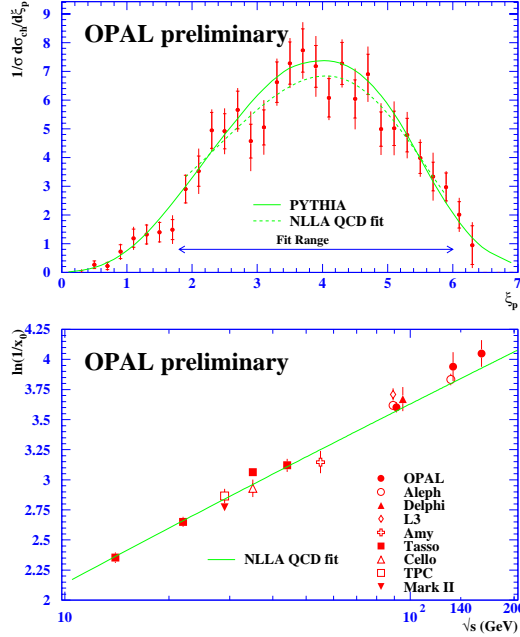


Figure 13: (a) The distribution of  $\xi_p$  as compared to PYTHIA from OPAL. The dashed curve is a NLLA fit. (b) The values of the peak position,  $\xi^*$  for several different energies and different experiments. The solid line is a fit to the NLLA QCD prediction.

sented by the CDF<sup>31</sup> collaboration. The Modified Leading Log Approximation (MLLA)<sup>32</sup> predicts a parton multiplicity scaling as a function of  $E_j\theta/Q_{eff}$  where  $E_j$  is the jet energy,  $\theta$  is the cone size, and  $Q_{eff}$  is an energy cut-off which delineates the edge of pQCD's descriptive capability for describing fragmentation.

As shown above, these measurements are standard fare for  $e^+e^-$  experiments, each performed at a different accelerator. The interesting feature of the CDF measurement is that by choosing well-balanced dijet events, different center of mass energies can be spanned. Then, at a given  $M_{jj}$ , with different cones, charged particles can be counted and  $\xi_p$  can be related in a complicated manner to  $E_j\theta/Q_{eff}$ . Figure 14 shows such a family of distributions for  $M_{jj} = 390 \text{ GeV}/c^2$ . From  $80 < M_{jj} < 600 \text{ GeV}/c^2$ , CDF can determine  $\xi^*$  as a function of “center of mass energy” and directly compare particle production from the hadron collider to that of  $e^+e^-$  experiments. Figure 15 shows a family of CDF measurements compared with measurements of TASSO, OPAL, and ALEPH. QCD measurements at the Tevatron are

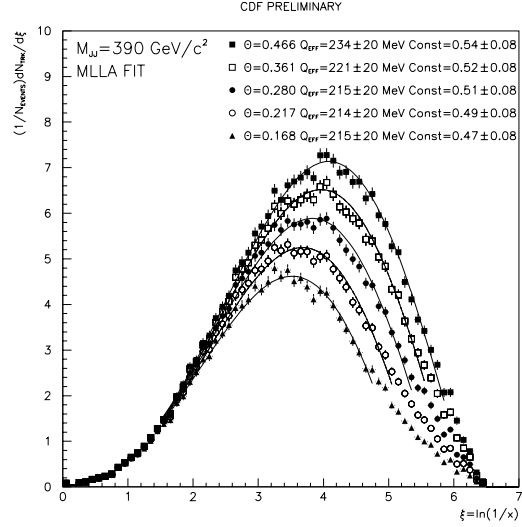


Figure 14: Inclusive momentum distributions of charged tracks inside jets for different opening angles at a single  $M_{jj}$  of  $390 \text{ GeV}/c^2$ .

indeed becoming very sophisticated.

#### 4.4 Dijet Production

Measurements of the properties of events with two jets are benchmark efforts which are beginning to yield benefits. The long reach of scale makes this important as both a physics and engineering tool. In the latter role, it is anticipated that by fixing  $E_T$  in the triple differential cross section,  $d\sigma/dE_T d\eta_1 d\eta_2$  that combinations of  $x_1$  and  $x_2$  can be constructed and eventually unfolded into pdf global fits. As is always the case with such delicate, long reach measurements, systematic uncertainties in the energy scale will dominate. Both CDF<sup>33</sup> and DØ<sup>34</sup> presented results on the mass distributions of dijet samples collected in the Run 1B exposure. Figures 16 and 17 show these cross sections. Note the systematic uncertainties are quite large at the highest masses of  $500\text{-}800 \text{ GeV}/c$ .

The nature of this fundamental “4 parton” annihilation process suggests that the angular distributions of the outgoing partons are strictly governed by the helicity arrangements. Any unusual propagator will likely show up as an unanticipated contribution to the density matrix. Specifically, a contribution which behaves as a contact term will

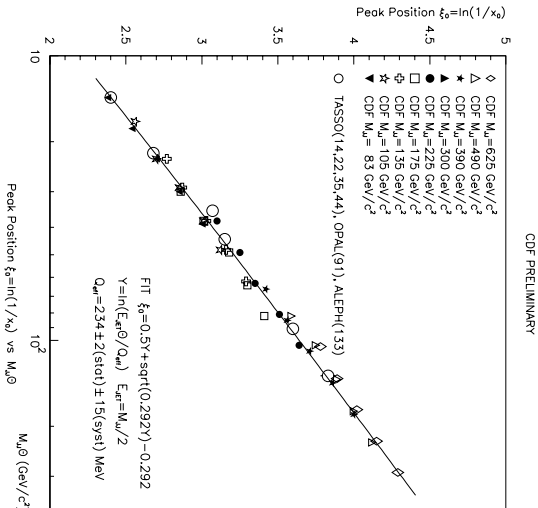


Figure 15: The evolution of the peak position,  $\xi^*$  as a function of  $M_{J\theta}$ . One can see that scaling is observed.

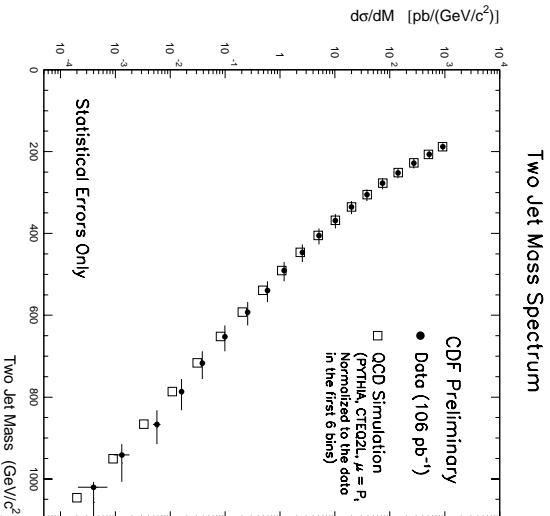


Figure 16: CDF dijet invariant mass distributions from run 1B.

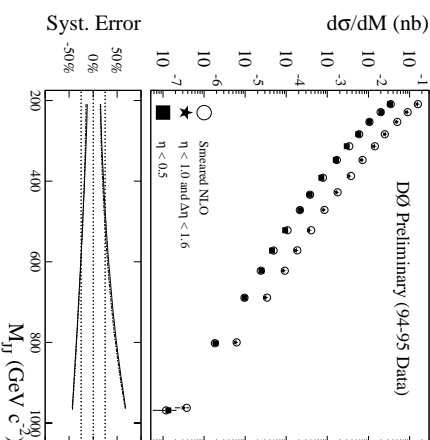


Figure 17:  $D\bar{O}$  dijet invariant mass distributions for run 1B. The insert shows the magnitude of the systematic uncertainties, dominated by the hadron energy scale.

lead to a flattening of the center of mass scattering angle,  $\theta^*$ . Therefore, strict predictions on the angular distributions of jets are available and can be checked.

The determination of  $\cos \theta^*$  is directly related to measurables through  $\cos \theta^* = \tanh \left[ \frac{\eta_1 - \eta_2}{2} \right]$ . Traditionally, the quantity,  $\chi = \frac{1 + \cos \theta^*}{1 - \cos \theta^*}$  is used. This is because  $\chi$  has the effect of de-emphasizing Rutherford scattering angles: the distribution at high  $\cos \theta^*$  is mapped to very low  $\chi$ . Figures 18 and 19 show the  $\chi$  distributions for dijet events from both CDF and  $D\bar{O}$ . This is a measurement which is unusually free of overwhelming scale uncertainties. Only any  $\eta$ -dependence of scale knowledge is important. (Also, multiple interactions are a potential problem.) Both sources of uncertainty are each at the 8–10% level. Note that there is good agreement with the NLO pQCD predictions for all distributions, suggesting that new physics which might manifest itself through a contact-like term is not apparent. CDF<sup>33</sup> sets a preliminary limit for the mass of a contact term of  $\Lambda^{+(-)} > 1.8(1.7)\text{TeV}/c^2$  at 95% C. L. where the signs indicate a constructive or destructive flavor symmetric left-hand term in the interaction.

#### 4.5 Scaled Inclusive Jet Cross Section

One of the persistent anomalies lies is the scaled cross section for inclusive jets observed by CDF. The issue is the degree to which scaling violations are observed in inclusive jet cross sections. UA<sub>2</sub><sup>15</sup>

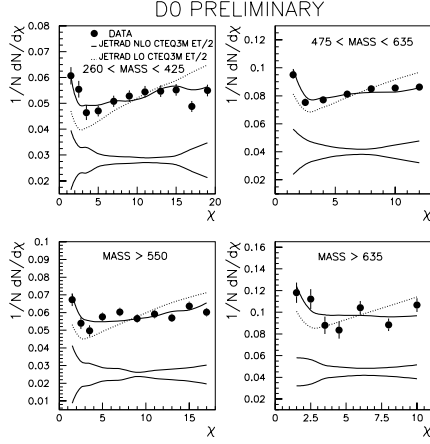


Figure 18:  $D\bar{D}$  dijet  $x$  distributions in different regions of  $M_{12}$ . The error bars are statistical, while the systematic uncertainty is represented as  $\pm 1\sigma$  bands. The curves are LO and NLO predictions of JETRAD using the CTEQ3M pdf's and a renormalization scale defined as  $E_T/2$ .

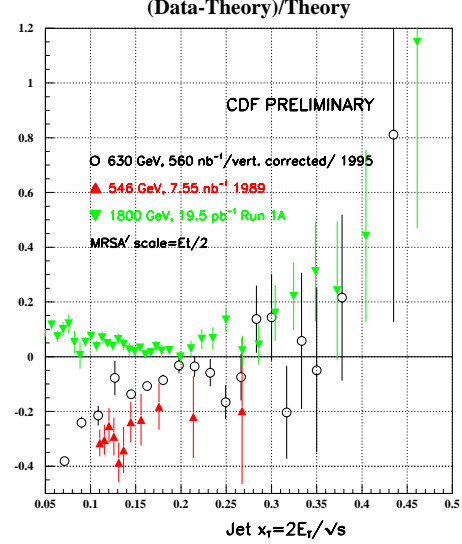


Figure 20: The difference between data and expectation for the CDF inclusive jet cross sections for all three exposures.

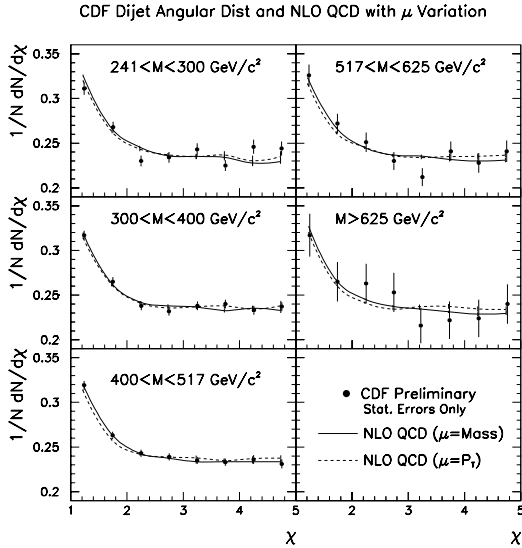


Figure 19: CDF dijet  $x$  distributions in different regions of  $M_{12}$ .

observed scaling violations which are consistent with predictions of pQCD. However, CDF found that, while the data taken at  $\sqrt{s} = 1800$  GeV fit NLO pQCD expectations, the early period of running at lower energy (546 GeV in 1989) did not fit the expectation. At this conference, preliminary results from the Run 1C data were shown which seem to confirm the earlier surprise. Figure 20 shows all three exposures in the ubiquitous linear presentation. While comparison with UA2 is complicated due to differences in jet algorithms and jet energy corrections, one might conclude that there appears to be a disagreement between the experiments. However, there is an overall relative normalization uncertainty and when this is taken into account, the apparent disagreement appears to be not serious in the kinematical region where the experiments overlap. The UA2 data were for  $x_T > 0.15$  and the CDF data extended below that to approximately  $x_T = 0.1$ , where most of the discrepancy with expectation is. The full analysis of the scaled cross sections was not presented. The  $D\bar{D}$  analysis of this running is not complete yet and so it is difficult to draw conclusions.

#### 4.6 Single Inclusive Jet Production

A particularly timely topic at this conference and one which has been both confusing and controversial for nearly a year was the measurement of the single inclusive jet cross section by both CDF and DØ and the comparison of those measurements with each other, and with NLO pQCD expectations. The stakes on the outcome of this measurement are very high, as history suggests new physics can emerge from probes of shorter and shorter distances. This is a particularly delicate probe of distances as short as  $10^{-17}$  cm. It is also a near-heroic measurement of over 10 orders of magnitude in  $d\sigma/dE_T$  up to  $E_T = 500$  GeV. The expectations of the NLO pQCD model are presumably well understood over that region. The sort of new physics which might cause a deviation from expectations in this measurement is related to the same sort of non-standard ingredient which is tested by the dijet  $\chi$  measurement. While nothing unexpected has appeared in these latter measurements, the Unusual could still emerge in the single inclusive jet cross section.

##### Status as of Summer 1996

The situation during the conference was the following. The CDF collaboration had published the preceeding week their analysis of the Run 1A exposure<sup>35</sup> which showed a statistically significant excess of events above the expectations... in just the interesting region. The DØ collaboration had similarly measured this cross section and found<sup>36</sup> no excess over the entire range of  $E_T^{jet}$ . The results from DØ are not published. The systematic uncertainties for both experiments are large... 30-50% in the region of interest, due primarily to jet scale uncertainties. For this conference, both experiments reported preliminary results for the Run 1B exposure. Figure 21 shows the two measurements from CDF Run 1A, CDF Run 1B<sup>33</sup>, and DØ Run 1B data<sup>37</sup>. The complication is in the comparison to the models of NLO pQCD.

The modeling of the physics is done differently by the two experiments: CDF uses the model of Ellis, Kunszt, and Soper<sup>38</sup> (EKS), while DØ uses the model of Giele, Glover, and Kosower<sup>39</sup> (JETRAD). The full story is not discernable on the logarithmic plot, and so all experiments resort to a linearized presentation,  $[D - M]/M$ , (borrowed

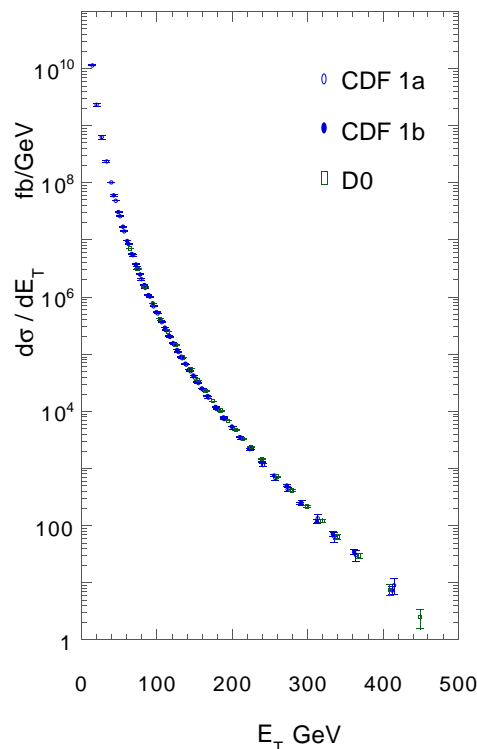


Figure 21: Inclusive cross section for CDF (1A, open circles; 1B, closed circles) and DØ (1B, open squares)

from direct photon analyses... or *vice versa*).

The source of possible excitement is shown in Figure 22. The source of confusion is shown in Figure 23. In Figure 22 one sees a clear indication of a rise in the cross section, over the NLO pQCD theory. This is a statistically significant rise, as detailed in the publication<sup>35</sup>. Figure 24 shows the detailed accounting which has been done by the CDF analysis on eight different correlated systematic uncertainties. These sum in quadrature to the insert at the bottom of Figure 22. While the systematics are a serious matter, none of them were found to be significant enough to account for the discrepancy and so the consistency of the rise and the magnitude of the discrepancy has led many to imagine that new physics could be the cause. DØ does not see such a rise, and comments that their systematics are not well enough understood to be able to make a claim of new physics. This situation begs for a systematic, reasoned look.

##### Three Questions:

In order to calibrate the situation, it is necessary to ask and answer three questions: 1) Do the data

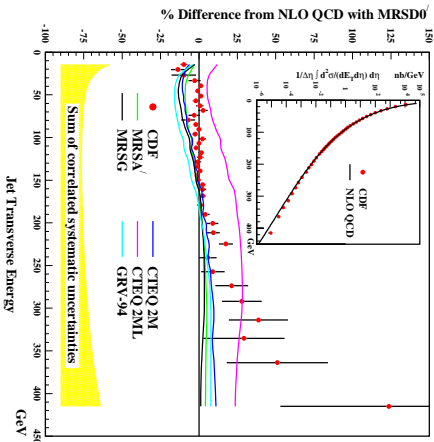


Figure 22: CDF measured inclusive cross section shown as  $[D - \text{EKS}]/\text{EKS}$ .

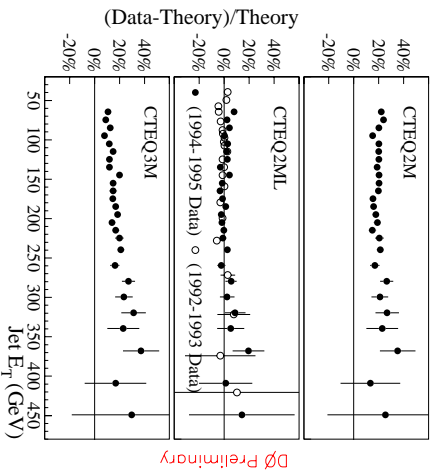


Figure 23:  $D\bar{D}$  measured inclusive cross section shown as  $[D - \text{JETRAD}]/\text{JETRAD}$

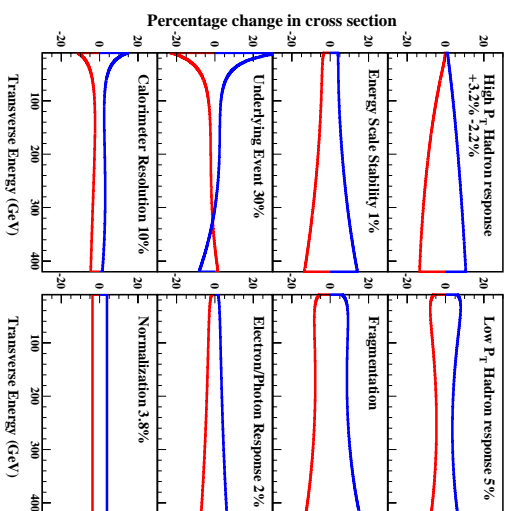


Figure 24: CDF determination of systematic uncertainties.

disagree? 2) Do the theories disagree? and 3) Do the models disagree? Each of these questions will be addressed in turn, but with an eye on better understanding the display of information. Figure 25 shows the same CDF data as in 21, but scaled in a manner which both emphasizes and linearizes the region of interest. The EKS model is shown as are the Run 1A and Run 1B data, all scaled by  $E_T^7$  and then reduced by  $10^{-19}$  in order to set a reasonable vertical scale. The excess is evident, but it is not necessary to make the confusing subtraction and subsequent “theory”-normalization in  $[D - M]/M$ . Figure 26 shows the same thing for the  $D\bar{D}$  data where the JETRAD model prediction is scaled upwards by 20% as is both allowable and customary by  $D\bar{D}$  in this particular comparison. No deviation from expectation is shown.

**Do the Experiments Disagree?** In order to compare the data, it is necessary to adjust one or the other set so that they are measuring the same quantity. The CDF measurement is made in the region of pseudo-rapidity,  $0.1 < |\eta| < 0.7$  while the  $D\bar{D}$  data make the measurement for jets accepted in the region  $|\eta| < 0.5$ . This adjustment is  $E_T$ -dependent and as much as a 20% reduction in cross section, in going from the  $D\bar{D}$  acceptance to that of CDF. Figure 27 show the two experimental measurements with the adjustment made to the

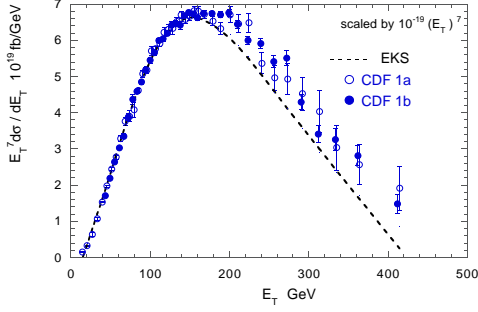


Figure 25: CDF 1A and 1B inclusive cross section data scaled by  $E_T^7$ .

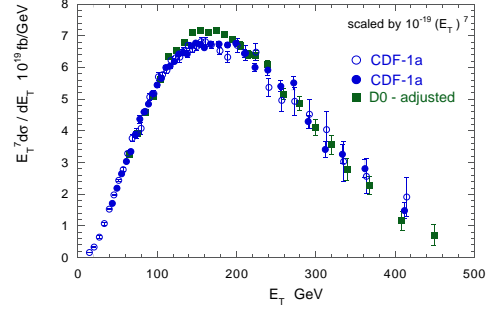


Figure 27:  $D\bar{D}$  and CDF scaled cross sections with  $D\bar{D}$  adjusted for the acceptance difference.

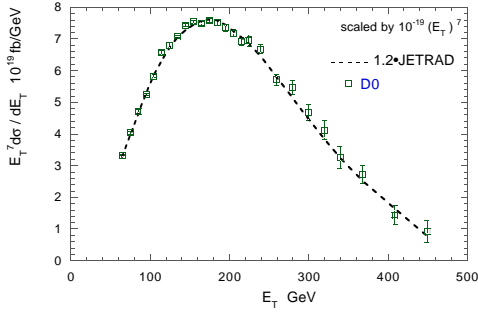


Figure 26:  $D\bar{D}$  measured inclusive cross section, scaled by  $E_T^7$  for the 1B exposure.

$D\bar{D}$  data. Note that each experiment quotes a nearly  $E_T$ -independent overall normalization uncertainty of 4-5%. With the overall systematic uncertainties in each, it is not possible to claim that these data disagree.

**Do the Theories Disagree?** This is not the right question. Both calculations use the same NLO pQCD theoretical formalism. The correct question is a different one.

**Do the Models Disagree?** The two models of pQCD and the experimental situations are different.

**CDF Model** The CDF analysis utilizes a computer code which is provided by the authors of EKS. It is a totally inclusive calculation, yielding the kinematics of a jet. This means that: all other jets are integrated over; a merging algorithm is applied; and a renormalization scale (=factorization scale),  $\mu$ , is defined. In this case, the only

practical definition is for  $\mu \equiv \beta E_T^{jet}$ , a fraction of the  $E_T$  of the jet. The experimenters control the value of  $\beta$  and the pdf which is used in the generation. The program is used exclusively at the parton level.

**$D\bar{D}$  Model** The  $D\bar{D}$  analysis also utilizes a computer code provided for them by the theoretical group responsible for the JETRAD program. This is a “phase space” monte carlo calculation in which all of the jets are generated in each event and the inclusive cross section is determined as in the experiment. There is no clustering enforced and  $\mu$  is defined as  $\mu \equiv \alpha E_T^{leading jet}$ . The experimenters control the clustering algorithm applied,  $\alpha$ , and the pdf used in the generation. The program is used exclusively at the parton level.

The clustering algorithm used by both experiments is the so-called fixed cone “Snowmass Accord”. This is implemented in a monte carlo simulation by asserting that partons cannot be clustered into a “jet” if they are more than  $2R_C$  apart, where  $R_C$  is the cone radius, here chosen to be  $R_C = 0.7$ . This is implemented directly by CDF. The  $D\bar{D}$  analysis uses the same approach, except it is modified to be not just  $R_C$ , but  $R_C \times \mathcal{R}_{sep}$  where  $\mathcal{R}_{sep} = 1.2$ , so widely-separated partons are less likely to be clustered in the  $D\bar{D}$  implementation. Because the JETRAD allows for a modification of the clustering algorithm, the  $E_T$  dependence of this difference can be calculated. Figure 28 shows this correction for  $\mathcal{R}_{sep} = 1.2 \rightarrow 2.0$ . Note that there is a decrease of acceptance of about 5% at low  $E_T$  for the  $D\bar{D}$  relative to the CDF approach.

The scale definition is obviously going to carry an  $E_T$  dependence. In EKS, the implementation is

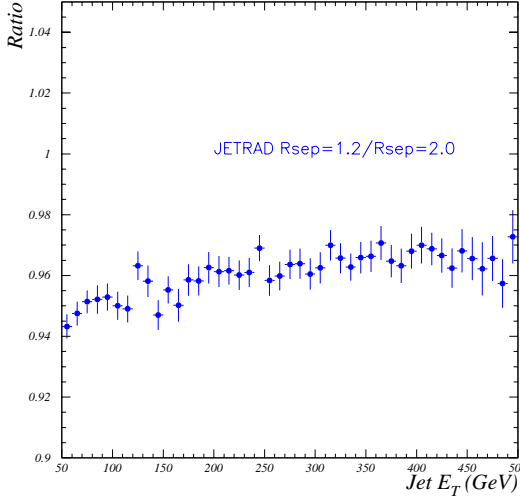


Figure 28: The difference between the cluster definitions used by DØ and CDF shown as a ratio.

fixed at  $\mu(\text{EKS}) = 0.5E_T^{jet}$ , while the DØ implementation of JETRAD has a scale definition set at  $\mu(DØ) = 0.5E_T^{leading jet}$ . JETRAD's flexibility allows it to be used in the EKS manner and the bottom plot in Figure 29 shows this difference. Again, there is a reduction in acceptance of about 10% at the lowest  $E_T$ . Both experiments and theorists agree that there is no overall  $E_T$  dependence associated with the value of  $\alpha$  or  $\beta$ ... the overall level of the predicted cross section changes. Also, note that there is no single correct choice for either  $\alpha$  or  $\beta$ —hence an overall normalization uncertainty for the model. This is shown in the top plot of Figure 29.

Finally, CDF most prominently published the experimental results compared with the MRSD0' pdf, while DØ concentrated on the CTEQ2M pdf. Each has explored other pdf effects, but the difference between these two is appropriate, given the controversy. Figure 30 shows the comparison for these pdf differences, again showing a decrease in acceptance of approximately 10% at the lowest  $E_T$  values.

Taken together, these three effects account for the  $E_T$  dependence in the overall model difference between the two analyses. Pretending that they are all independent, a combination of the three results in an overall adjustment which could be

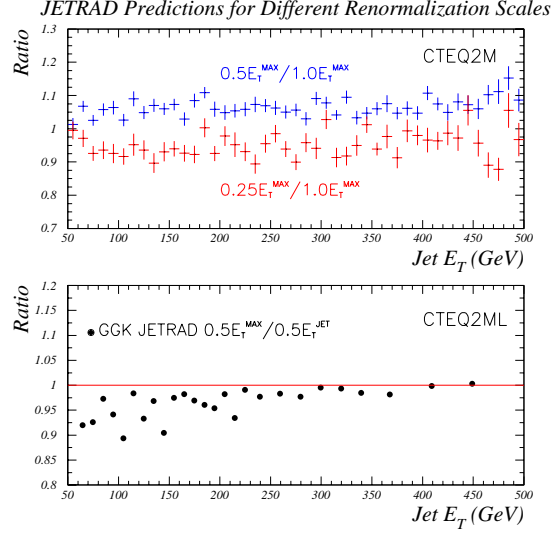


Figure 29: The difference between the scale definitions used by DØ and CDF shown as a ratio (bottom). In the top plot, the  $E_T$  insensitivity to the overall value of  $\alpha$  is shown.

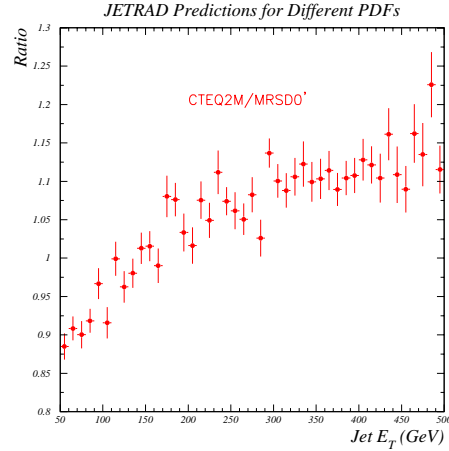


Figure 30: The difference between the pdf sets prominently used by DØ and CDF shown as a ratio.



applied to a  $D\bar{D}$ -like model to mimic a CDF-like model. When this is done, there can be adjustment of 40% upwards at 400 GeV for an initially flat  $[D - M]/M$ ! Given the overall scale uncertainty associated with the value of  $\beta$ , one begins to become suspicious that the controversy about two experiments may reduce to simply the difference between the two independent models used by the two experiments. A more sophisticated analysis of the sort done here should probably result in an additional *model systematic uncertainty* which might mitigate the confusion.

### So, How About the Gluon Density?

In recent years, knowledge of the gluon distribution has become considerably more precise. The low  $x$  data of HERA have supplemented the medium  $x$  data from direct photon experiments and deep inelastic scattering. The issue of how well  $G(x)$  is understood at  $x$  values which are relatively high is directly relevant to the issue of inclusive jets. At Fermilab, a jet with  $E_T = 300$  GeV is produced at  $x \sim 0.3$  and fully a quarter of jet production occurs with gluons of that value.

Among the attempts to understand the apparent discrepancy, some confusion has emerged regarding the ability of the gluon distribution to accommodate the inclusive jet data excess. A recent analysis by the MRS group<sup>40</sup> shows that it is impossible to accommodate the jet data with the allowed  $G(x)$  and that parton distributions are not a likely source of explanation. Coincident with this analysis, indeed published in the same issue of Physical Review Letters<sup>41</sup> as the CDF paper, the CTEQ collaboration came to the opposite conclusion regarding  $G(x)$ . They found that the addition of a more flexible parameterization in the  $f(x)$  term of equation 2 results in a good fit with the rest of the DIS data... while simultaneously accommodating a 20-25% increase in the inclusive jet cross sections at the highest  $E_T$ .

Very recently, the CTEQ collaboration expanded their global fitting into a new iteration, CTEQ4<sup>42</sup>. These fits incorporated new muon DIS results, new HERA results, the jet data from both CDF and  $D\bar{D}$ , and the flexibility in  $G(x)$  referred to above. Furthermore, they intentionally over-weighted the high  $E_T$  inclusive jet data as a test to see whether a consistent set of pdf's could still be produced.

Reliance on pdf global fitting to answer fundamental questions, or point toward or away from new physics, requires care. It is important to understand that all global fitting is done with a measure of adjustment based on experience and caution. The reasons for this are obvious: of the 1297 dof in the CTEQ fits, 1168 are data points from deep inelastic scattering. The ability of specialized data to influence those fits is nil without some unusual attention. For example, the Drell Yan asymmetry data which directly affect the difference of up and down sea distributions contribute only 1 data point; the CDF  $A^W(y)$  data contribute 9 data points; and the Tevatron jet data provide only 62 points. The CTEQ approach is to weight these important, but sparse data by enhancing their relative contributions. Operationally, the two asymmetry contributions are treated as if their statistical errors are smaller than they are. Likewise, the single inclusive jet data statistical errors are similarly weighted.

Figure 31 shows the results of the CTEQ4M fits as applied to the familiar  $[D - M]/M$  linear plots. Beware: This is yet another analysis of the experiments, but now by the CTEQ group using only EKS...they are not the same as the experimenters' presentations. A further difference from the "stock" presentations is the fact that CTEQ allows the normalizations to float. One can see the same conclusion is reached as in the previous paragraphs: there is little difference between the data and a model.

However, because there is still a hint of excess, the CTEQ group did a test. They further emphasized the high data above  $E_T > 250$  GeV by reducing the statistical errors even more, leaving the data below 250 GeV reduced by the original factor. These fits are termed the "CTEQHJ" fits and are not necessarily meant to be a part of the standard CTEQ4 portfolio. Rather, they are a demonstration that a quality fit can be extracted which eliminates by construction the high  $E_T$  effect. Figure 32 shows the linearized presentation for these fits. The quality of the CTEQ4M and CTEQHJ fits is nearly identical, with  $\chi^2/\text{dof} = 1320/1297$  for the former, and  $\chi^2/\text{dof} = 1343/1297$  for the latter.

Finally, in preparation for this meeting, an unofficial CTEQ<sup>43</sup> fit was performed in which the data were *shifted* up by 3 statistical  $\sigma$ 's and then weighted by the original CTEQ4M factor as before. These fake, high- $E_T$ -emphasized data give a fit

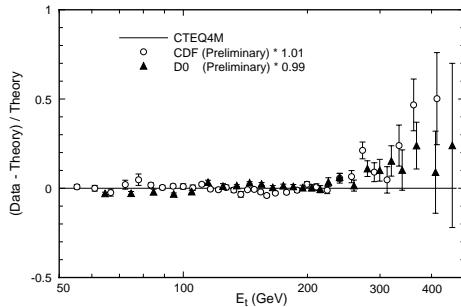


Figure 31: The linear presentation of CDF and DØ data as calculated by the CTEQ collaboration with the CTEQ4M pdf set. Note that the normalization is allowed to float.

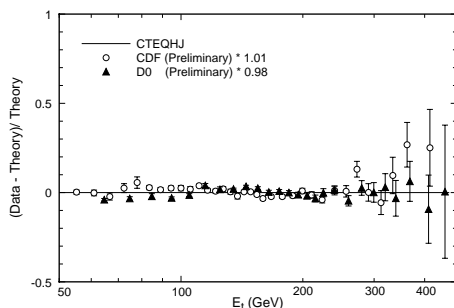


Figure 32: Same as Figure 31, except for the CTEQ4M set.

which is identical to the CTEQ4M fits, suggesting that there is a considerable leniency to the use of the weighting factors with jet data that are statistically not very precise.

### Inclusive Jet Conclusions

There are at least four conclusions that one can draw from this episode.

1. The models are sufficiently different, both inherently and in their implementation, to complicate drawing conclusions regarding new physics.

2. There is far more flexibility in  $G(x)$  than was originally thought and that flexibility is directly related to the kinematics of high  $E_T$  jets at Fermilab. The hints of discrepancy between theory and data in the direct photon analyses undoubtedly propagate into a theoretical uncertainty in their implementation as pdf ingredients... which further increases the care and caution required in order to interpret the single jet data and their agreement with pQCD.

3. Parton distributions are engineering tools, they require care and understanding in their use and in their interpretation.

4. Whether one attempts to reconcile one experiment's model with the other (done schematically here), or does a self-consistent analysis of both experiments with one model (done by CTEQ), one reaches basically the same conclusions: The data of the two experiments seem consistent and the flexibility in the physics modeling is too broad to reliably draw conclusions about new physics.

### 5 Conclusion

One cannot help but be impressed with the quality of the analyses of the Tevatron experiments, digging into the details of strong physics. In many analyses, the types of questions and analysis techniques are approaching the precision of  $e^+e^-$  experiments. While there is impressive agreement with much of pQCD, there are two outstanding issues which will hopefully become better understood by the Rochester Conference of 1998. Both issues are sticky—they involve the glue. First, the precision of the  $G(x)$  determination will clearly have to get better and the flexibility which appears inherent must be mitigated or eliminated. This will require a more careful understanding of the analysis of direct photon experiments, new ones as well as classical experiments. Certainly, a proper characterization of the theoretical uncertainties in the pdf analyses related to the apparent need for a primordial  $k_T$  smearing should be included. The second issue is the broad one of resummation. A consistent theory for the relevant low- $x$  radiation in both direct photon physics and Drell Yan production will be helpful. Certainly, additional QCD data will soon be available from the Tevatron experiments to shed light on these subjects... and maybe the Unexpected as well.

### Acknowledgements

I am grateful to a number of people who provided me with information in the preparation of this review. I would like to thank G. Blazey, A. Bodek, A. Brandt, T. Devlin, B. Flaugh, H. L. Lai, P. Melese, L. Nodulman, A. Para, H. Schellman,

W. K. Tung, H. Weerts, N. Varelas, and J. Womersley. It is a pleasure to thank the organizers of this conference and to acknowledge the splendid pre-conference arrangements for accessing submitted material. This work is sponsored by the National Science Foundation through NSF grant PHY-9514180.

## References

1. F. Abe *et al.*, Phys. Rev. Lett. **74**, 850 (1995); F. Abe *et al.*, Phys. Rev. Lett. **68**, 1458 (1992.)
2. A. Bodek, "Quarks and Gluons at Hadron Colliders", this conference.
3. W. Giele, E. Glover, and A. Kosower (DYRAD) Nucl. Phys. **B403**, 633 (1993.)
4. A. D. Martin, R. G. Roberts, and W. J. Stirling RAL-93-077 (1993).
5. A. D. Martin, R. G. Roberts, and W. J. Stirling RAL-94-055 (1994).
6. (CTEQ2M) J. Botts, *et al.*, Phys. Lett. **304B**, 159 (1993.)
7. (MRSA) A. D. Martin, R. G. Roberts, and W. J. Stirling, Phys. Lett. **B354**, 155 (1995.)
8. (CTEQ3M) H. L. Lai *et al.*, Phys. Rev. **D51**, 4763 (1995.)
9. S. Abachi *et al.*, Phys. Rev. Lett. **75**, 1456 (1995.)
10. F. Abe *et al.*, Phys. Rev. Lett. **76**, 3070 (1996.)
11. S. Abachi *et al.*, "Production Properties of  $W$  and  $Z$  Bosons at  $D\bar{O}$ ", submitted to this conference.
12. J. Collins and D. Soper Nucl. Phys. **B193**, 381 (1981), Nucl. Phys. **B197**, 446 (1982), E Nucl. Phys. **B213**, 545 (1983); J. Collins, D. Soper, and G. Sterman Nucl. Phys. **B250**, 199 (1985), J. Collins and D. Soper, Phys. Rev. **D16**, 2219 (1977.)
13. C. Balazs, J. Qui, C. P. Yuan (RESBOS) Phys. Lett. **B355**, 548 (1995.)
14. G. A. Ladinsky and C. P. Yuan Phys. Rev. **D50**, 4239 (1994); C. Davies and W. J. Stirling, Nucl. Phys. **B244**, 337 (1984) and C. Davies, B. Webber, and W. J. Stirling, Nucl. Phys. **B256**, 413 (1985.)
15. E. L. Berger and H. Contopanagos "Perturbative Resummation of the Top Quark Cross Section in Hadron Reactions", submitted to this conference; E. Berger and H. Contopanagos, Phys. Lett. **B361** (1995) 115 and Erratum; E. Laenen, J. Smith, and W.L. van Neerven, Nucl. Phys. **B369** (1992) 543, E. Laenen, J. Smith, and W.L. van Neerven, Phys. Lett. **B321** (1994) 254; and S. Catani, M. Mangano, P. Nason, and L. Trentadue, CERN report CERN-TH/96-21. ANL-HEP-CP-95-85 (hep-ph/9512212), to be published in the Proceedings of the International Symposium on Heavy Flavor and Electroweak Theory, Beijing, August, 1995.
16. P. Arnold and R. P. Kauffman Nucl. Phys. **B349**, 381 (1991.)
17. L. Nodulman "Direct Photons at CDF", submitted to this conference.
18. S. Abachi *et al.*, "Direct Photon Measurements by the  $D\bar{O}$  Experiment", submitted to this conference.
19. H. Baer, J. Ohnemus, and J. F. Owens, Phys. Rev. **D42**, 61 (1990.)
20. J. Huston *et al.*, Phys. Rev. **D51**, 6139 (1995.)
21. H. Baer and M. H. Reno, "Multiple Parton Emission Effects in Next-to-Leading Order Direct Photon Production", hep-ph/9603209, 1996.
22. E. Bonvin *et al.*, Phys. Lett. **B236**, 523 (1990.)
23. M. Zielinsky, "Results from E706 at Fermilab", submitted to this conference.
24. OPAL, "A test of QCD shower models with photon radiation from quarks", submitted to this conference.
25. UA1: M. Lindgren *et al.*, Phys. Rev. **D45**, 3038 (1992), UA2: J. Alitti *et al.*, Phys. Lett. **B263**, 563 (1991.)
26. S. Abachi *et al.*, "A Measurement of the Ratio of  $W + 1$  jet to  $W + 0$  jet Cross Sections and Comparisons to QCD", submitted to this conference. See also, S. Abachi *et al.*, Phys. Rev. Lett. **75**, 3226 (1996.)
27. S. Abachi *et al.*, Fermilab-Conf-95/182-E, and F. Abe *et al.*, Phys. Rev. **D50**, 5562 (1994.)
28. S. Abachi *et al.*, "Color Coherence" in  $p\bar{p}$  Collisions at  $\sqrt{s} = 1.8$  TeV", submitted to this conference.
29. The OPAL Collaboration, "Initial Studies of hadronic events at 161 GeV at LEP 2", submitted to this conference.

30. C. Fong and B. Webber, Nucl. Phys. **B355**, 54 (1991.)
31. A. Korytov, "Inclusive momentum distributions of charged particles in jets at CDF", submitted to this conference.
32. Y. Dokshitzer, V. Khoze, A. H. Mueller and S. Troyan, *Basics of Perturbative QCD*, Editions Frontieres, France, 1991.
33. T. Devlin "QCD Physics at CDF", presented at this conference.
34. S. Abachi *et al.*, "The Dijet Mass Spectrum and Angular Distributions with the DØ Detector", submitted to this conference.
35. F. Abe *et al.*, Phys. Rev. Lett. **77**, 438 (1996.)
36. J. Blazey "The Inclusive Jet Cross Section and Dijet Mass Distribution", XXX<sup>st</sup> Rencontre de Moriond, March, 1996.
37. S. Abachi *et al.*, "Inclusive Jet Cross Section in  $p\bar{p}$  Collisions with the DØ Detector", submitted to this conference.
38. (EKS) S. Ellis, Z. Kunszt, and D. Soper, Phys. Rev. Lett. **64**, 2121 (1990) and F. Aversa, P. Chiappetta, M. Greco, and P. Guillet, Phys. Rev. Lett. **65**, 410 (1990.)
39. (JETRAD) W. T. Giele, E. W. N. Glover, and D. A. Kosower, Phys. Rev. Lett. **73**, 2019 (1994.)
40. E. W. N. Glover, A. D. Martin, R. G. Roberts, and W. J. Stirling, Phys. Lett. **B381**, 353 (1996).
41. J. Huston *et al.*, Phys. Rev. Lett. **77**, 444 (1996.)
42. H. L. Lai *et al.*, "Improved Parton Distributions from Global Analysis of Recent Deep Inelastic Scattering and Inclusive Jet Data", MSUHEP-60426, CTEQ-604, June 1996.
43. H. L. Lai and R. Brock, unpublished.
44. F. Abe *et al.*, Phys. Rev. Lett. **70**, 1376 (1993).
45. J. A. Appel *et al.*, Phys. Lett. **B160**, 349 (1985).

## Questions

*B. Kniehl, MPI Physik Munich:* Comment: There is a significant theoretical uncertainty in the NLO calculation of single jet inclusive production at the Tevatron in the high  $E_T$  range due to the  $\overline{\text{MS}}$ -DIS scheme dependence (see the recent analysis by M. Klasen and G. Kramer). In fact, the CDF data

agree reasonably well with the NLO prediction in the DIS scheme.

*R. Brock:* Yes, there could indeed be factorization-scheme dependence in the application of a model to these data. The work referred to (hep-ph/9605210) does an analysis using the DIS pdf set, CTEQ3D which is functionally equivalent to the  $\overline{\text{MS}}$ CTEQ3M. However, while the DIS scheme precisely defines the quark distributions, it does not do so for the gluon distribution. This is fixed by convention. So, here again, we find that there is possibly a gluon-component to our flexibility in interpreting these data, hidden inside of our inherent flexibility in defining how to deal with a finite perturbative expansion. The agreement that these authors find is indeed intriguing, but I don't think necessarily inconsistent with the recognition that there are overall uncertainties in the models and the use of and values for the gluon distributions.

*G. Willi, SINS Warsaw:* Did models you reported dealing with the large  $E_T$  excess include multiparton rescattering? Comment: Some time ago in cosmic rays a similar excess has been reported and the analysis used a contact term  $\Lambda = 1.7$  TeV, very near to your  $\Lambda = 1.6$  TeV.

*R. Brock:* No, this was not included in the models. Regarding your comment: I was not aware of this. However, the uncertainties in analyzing cosmic ray physics results must also be quite significant and I would not be prepared to imagine yet that, given the above situation, this offered a better explanation.

*J. Phillips, Liverpool University/PPARC:* What is the range in  $t$  and  $x_T$  covered by the CDF "Tokyo" pot devices?

*R. Brock:* The best acceptance is for  $|t| < 1$  GeV/c<sup>2</sup> with  $\xi_p \sim 0.05 - 0.1$ . At higher  $|t|$  the backgrounds become significant. At the mean  $E_T \sim 15$  GeV for dijets,  $x_T \sim 0.053 - 0.075$ . (Thanks to P. Melese for information.)